THE JOURNAL OF PHYSICAL CHEMISTRY A

Article

pubs.acs.org/JPCA

Remarks on the Validity of the Fixed Nuclei Approximation in Quantum Electron Dynamics

Inga S. Ulusoy and Mathias Nest*

Theoretische Chemie, TU München, Lichtenbergstrasse 4, 85747 Garching, Germany

ABSTRACT: In this paper we report quantum dynamical simulations that test the fixed nuclei approximation, which is usually invoked in ab initio correlated electron dynamics. We do so by employing a recently developed method, called multiconfiguration electron nuclear dynamics. Additionally, we discuss the influence of the multiconfiguration expansion length on the results.

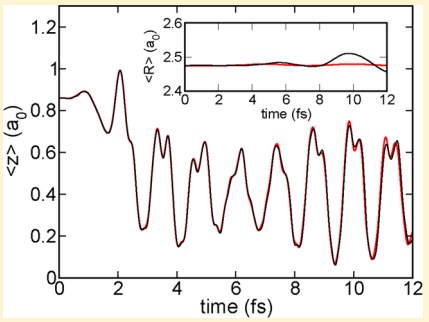

1. INTRODUCTION

Most simulations of the correlated quantum dynamics of electrons in recent years have been done in the so-called fixed nuclei approximation. The reason for this approximation has been that the computational effort for a combined propagation of electrons and nuclei is very high, especially if electronic wave packets are created that span a large number of potential energy surfaces. The justifaction for this approximation is that usually the electrons move on a time scale that is 100 times shorter than the time scale of the atoms, so that most of the interesting electron dynamics is over when nuclear motion sets in. For certain situations it was possible to even treat moving nuclei, e.g., using mixed quantum classical approaches,[1−3] electron−nuclear dynamics (END) methods,[4−8] or standard nonadiabatic quantum dynamics.[9−13]

As a newer attempt, efforts have been made recently to describe electrons and atoms on the same footing, i.e., to directly propagate the wave function of a molecule, instead of only parts of it. This development can either be seen as a multiconfiguration extension of the END method mentioned above, or as a variant of the multiconfiguration time-dependent Hartree method (MCTDH),[14−16] with build-in antisymmetrization of the electronic part of the wave function.[17−20] To distinguish between the more general MCTDH method and the present method, we refer to it as multiconfiguration END (MCEND).[21−23] Here, the time-dependent Schrödinger equation

$$\dot{\Psi} = -\frac{i}{\hbar} H_{\mathrm{mol}} \Psi \tag{1}$$

is solved for a *molecular* Hamiltonian

$$H_{\mathrm{mol}} = T_e + T_n + V_{ee} + V_{nn} + V_{en} \tag{2}$$

This gives us access to the full END, and thus permits us to test the validity of the fixed nuclei approximation. Also, this will give us the possibility to further explore the properties of MCEND, which is a quite young method. Given that most quantum dynamical simulations are still done for systems with less than 10 degrees of freedom (dof; with a few exceptions), propagating a molecular wave function is still a formidable task. For this reason we have chosen the LiH molecule, which has 12 spatial electronic dof and one nuclear dof.

The paper is organized as follows. The next section gives a brief description of the theory, section 3 presents the results of our simulations, and section 4 summarizes this paper.

2. THEORY

The MCEND wave function[21−23] is an MCTDH type wave function,[14−16] which contains an explicitly antisymmetric part for the electrons. In other words, it is a sum of products of determinants $\det_{J_e}$ and Hartree products. The determinants are built from the n_e spin orbitals $\phi^e_{j_i}(\vec{x}_i, t)$ (SOs), with $\vec{x}_i$ denoting the spatial and spin coordinates of electron i, from a total of N_e electrons.

$$|\det_{J_e}(\{\vec{x}_i\}, t)\rangle = |\phi^e_{j_1^e}(\vec{x}_1, t), \phi^e_{j_2^e}(\vec{x}_2, t), \ldots, \phi^e_{j_{N_e}^e}(\vec{x}_{N_e}, t)\rangle \tag{3}$$

Each determinant can be identified by an N_e-tuple $J_e = (j_1^e, j_2^e, \ldots, j_{N_e}^e)$ of indices of the SOs.

The nuclear part Φ_{J_n} of the wave function is made of Hartree products of n_k single-particle functions $\phi^{n,k}_{j_k^n}(R_k,t)$ (SPFs) for the kth dof.

$$\Phi_{J_n}(\{R_i\}, t) = \prod_{k=1}^{N_k} \phi^{n,k}_{j_k^n}(R_k, t) \tag{4}$$

N_k denotes the $3N - 6(5)$ dof with N being the number of atoms, and the number 5 in parentheses holds for linear molecules. Each product is identified by an N_k-tuple $J_n = (j_1^n, j_2^n, \ldots, j_{N_k}^n)$ of indices of the SPFs.

Special Issue: Jörn Manz Festschrift

Received: April 30, 2012
Revised: June 18, 2012
Published: June 18, 2012

dx.doi.org/10.1021/jp304140r | J. Phys. Chem. A 2012, 116, 11107−11110

The MCEND wave function is then expressed as

$$|\Psi(\{\vec{x}_i\}, \{R_i\}, t)\rangle = \sum_{J_e}^{\text{ord}} \sum_{J_n} A_{J_eJ_n}(t)|\det_{J_e}(\{\vec{x}_i\}, t)\rangle |\Phi_{J_n}(\{R_i\}, t)\rangle \quad (5)$$

The time-dependent coefficients $A_{J_eJ_n}(t)$ reflect the occupation of a given configuration. The sum over determinants is restricted to ordered J_e because of the permutational symmetry of the determinants. This leaves a total of $\binom{n_e}{N_e}$ determinants. The number of Hartree products is $\Pi_k {}^{N_k}_{=1} n_k$ because we assume distinguishable particles. Depending on the number of SOs and SPFs included, various expansion lengths of the MCEND wave function can be built. In the following, we denote the expansion length by $(n_e/2, n_k)$. Thus, for LiH with four electrons, an expansion length of (2,1) corresponds to the Hartree−Fock (HF) wave function with one nuclear SPF. The more SOs and SPFs are included in the wave function, the more electron and nuclear correlation is gained.

In order to describe electronic and nuclear wave packets simultaneously, it is necessary to construct the underlying basis in a special way. We begin as usual and write the MOs as linear combinations of Gaussian type orbitals, and the SPFs are represented on a grid. What is different in MCEND is that the electronic basis is not centered simply on the nuclei. Because of the width of the nuclear wave function, we have to place the same basis functions at several positions of "ghost atoms". The position of the ghost atoms are chosen such that they are close to the equilibrium geometry of the molecule while the overlap between the Gaussian type basis functions is kept minimal. We thus obtain a larger electronic basis than is implied by its name, 6-31G**. In a sense, this is a product basis of the nuclear dof with a single electronic dof. Unfortunately this large basis contains (near) linear dependencies, which need to be removed. For this, we use the canonical orthogonalization as described in the book by Szabo and Ostlund.[24]

The equations of motion (EOM) for the SOs, the SPFs, and the coefficients are derived in close analogy to the MCTDH[15] and MCTDHF EOM. As they have been described in detail in previous papers,[21,22] we will give them here only briefly for reference. The EOM of the coefficients are

$$\dot{A}_{J_eJ_n} = -i \sum_{L_e}^{\text{ord}} \sum_{L_n} \langle \det_{J_e} \Phi_{J_n}|H_{\text{mol}}|\det_{L_e} \Phi_{L_n}\rangle A_{L_eL_n} \quad (6)$$

which is a linear equation and comparatively easy to solve. The one- and two-electron integrals needed for the electronic matrix elements were calculated using the Gamess software package.[25]

The EOM for the SOs and SPFs are

$$\dot{\phi}^e = -i(1 - P^e)(\rho^e)^{-1}\langle H_e + V_{en}\rangle \phi^e \quad (7)$$

$$\dot{\phi}^n = -i(1 - P^n)[T_n + V_{nn} + (\rho^n)^{-1}\langle V_{en}\rangle]\phi^n \quad (8)$$

Here, we adapted a vector notation for the SOs with $\phi^e = (\phi^e_1, \phi^e_2, ..., \phi^e_{N_e})^T$. The operators P^x are projectors on the space spanned by the orbitals/SPFs, respectively. For a detailed discussion of the EOM, please see ref 15. Both are highly nonlinear, and rather difficult to integrate, among other things, because of the inverse of the density matrix. Also, the evaluation of the right-hand-side is computationally quite expensive, because a four-index-transform has to be done multiple times per time step.

3. RESULTS

As outlined in the Introduction, we will now look at the influence of nuclear motion on an electronic wave packet in different situations. In all cases, we began the propagation from the correlated ground state, which was obtained by propagation in imaginary time. Then an ultrashort laser pulse was used to excite the molecule, described in the dipole approximation

$$V_{\text{dip}} = -\sum_i \vec{r}_i\vec{E}(t) + \sum_A Z_A\vec{R}_A\vec{E}(t) \quad (9)$$

where the electric field has the form

$$\vec{E}(t) = \vec{E}_0 \sin^2\left(\frac{\pi}{2\sigma}t\right)\cos(\omega_0 t) \quad (10)$$

The pulse duration was always $2\sigma = 4$ fs, and the polarization along the z axis (the molecular axis). The field strength and carrier frequency were varied a little between different calculations, and will be reported below. However, the frequency was always high enough so that the coupling to the nuclear dipole moment could have been neglected.

We begin the presentation of our calculations with a (3,1) expansion length of the wave function, which means that the four electrons are distributed among three spatial orbitals, resulting in 15 determinants, and the single nuclear dof is described using one single particle function. This wave function is equivalent to a product ansatz for electronic and nuclear dof. The field strength and the frequency of the laser pulse were $E_{0,z} = 0.02\ E_h/e_0a_0$ and $\hbar\omega = 3.27$ eV, respectively. The latter is roughly in resonance with the first excited $^1\Sigma^+$ state, which also has a significant transition dipole moment along the molecular axis (z).[26] The laser pulse results in an energy uptake of 1.83 eV, which is a bit more than half the photon energy. Figure 1 shows the position

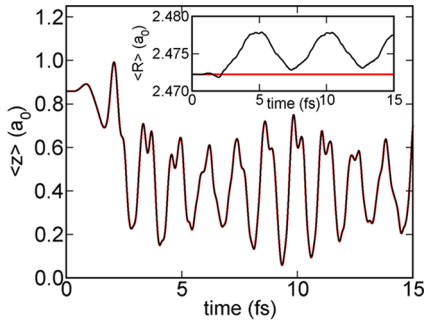

Figure 1. Electronic and nuclear (inset) position expectation values along the molecular axis of LiH for an expansion length of (3,1). Black: MCEND calculation; the nuclei can be seen to start oscillating in the inset. Red: Fixed nuclei ($\dot{\phi}^n = 0$) approximation.

expectation values along the molecular axis, $\langle z\rangle$ for the electrons and $\langle R\rangle$ for the nuclei, as a function of time. The nuclei begin a small amplitude motion very early, but energy is transferred to the nuclei only slowly (black line). Next, to simulate the fixed nuclei approximation, we set $\dot{\phi}^n = 0$ in our program, and repeated the calculation (red line). The nuclear position expectation value is now time-independent, but there is almost no difference in the electronic wave packet. Here, we have probably two effects, which amplify each other: The mean field nature of the ansatz of the wave function leads to a very small energy transfer to the

dx.doi.org/10.1021/jp304140r | J. Phys. Chem. A 2012, 116, 11107−11110

nuclear dof, and the small amplitude motion of the nuclei of less than 0.01 a_0 does not disturb the motion of the electrons very much.

To test this last point, we now proceed to an expansion length of (3,2), which means again 15 determinants for the state of the electrons, but now two single particle functions for the nuclear dof. This allows correlation between the electrons and the nuclei. Using the same laser pulse as before, we now find the oscillations shown in Figure 2. The nuclear oscillations are larger by about a

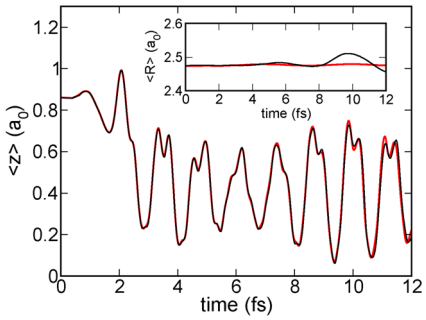

Figure 2. Electronic and nuclear (inset) position expectation values along the molecular axis of LiH for an expension length of (3,2). Black: MCEND calculation, the nuclei can be seen to start oscillating in the inset. Red: Fixed nuclei ($\dot{\phi}^n = 0$) approximation.

factor of 10 (black line), but still comparatively small. If we now apply the fixed nuclei approximation, by setting $\dot{\phi}_j^n = 0$, we find that the nuclear position expectation value is now *not* time-independent (red line), because the ϕ_1^n and ϕ_2^n have different centers, and their relative weight in the wave function can be changed by the coefficient vector $A_{JJ_n}(t)$. Still, this effect is small enough to accept this as being very close to stationary nuclei. Additionally, we find that the lines for the electron position expectation values are not superimposed anymore at later times.

Next, we performed simulations for a situation where the nuclei are not in their ground state at time $t = 0$. Instead we constructed a nuclear wave packet

$$\phi^n(R, t = 0) = \frac{1}{\sqrt{2}}(\chi_1(R) + \chi_m(R)) \tag{11}$$

where the χ_i are two eigenfunctions of the electronic ground state potential energy surface (PES). It should be noted that such a surface exists only if only one nuclear single particle function is used. Then, a potential can be derived from the ground state nuclear SPF ϕ^n, which in turn is obtained via propagation in imaginary time. The PES follows from

$$V_n(R) = -\frac{T_n\phi^n(R)}{\phi^n(R)} \tag{12}$$

which is just a rearrangement of the time-independent Schrödinger equation, and where T_n is the operator for the nuclear kinetic energy. Diagonalization of the effective nuclear Hamiltonian $T_n + V_n$ then gives the vibrational eigenstates χ_i.

Now we will compare how far such an oscillating nuclear wave packet will affect the electronic motion. For this we use an expansion length of (4,1), corresponding to 70 determinants. Also, the laser parameters have been changed slightly to $E_{0,z} = 0.025\ E_h/e_0a_0$ and $\hbar\omega_0 = 3.40$ eV. Figure 3 shows three cases: For the simulation shown in black, the nuclei were in their ground state and kept fixed, the red line corresponds to $m = 2$ in eq 11, and the blue line corresponds to $m = 4$. Clearly, the deviations of the

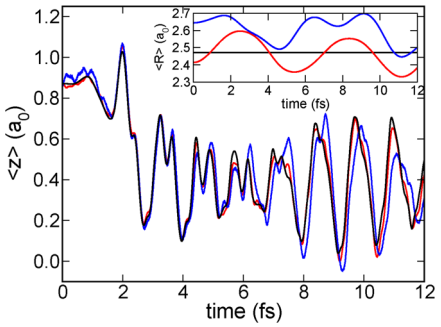

Figure 3. Position expectations for an MCEND (4,1) wave function, with fixed nuclei (black), and a vibrational wave packet (see eq 11) with $m = 2$ (red) and $m = 4$ (blue).

electronic position become stronger with increasing vibrational motion of the nuclei. This indicates one reason for the very small difference between the results shown in Figure 1: The nuclei have to acquire enough momentum and start to move before the dephasing sets in. Not so clear is the origin of the fast "quiver" motion of the electrons during the first femtosecond, and their disappearance at later times. It turns out that this comes from the fact that the electrons are at time $t = 0$ in a ground state corresponding to nuclei in their equilibrium geometry, although the nuclear wave function has been changed to a wave packet. To illustrate this point, we show in Figure 4 what happens if no

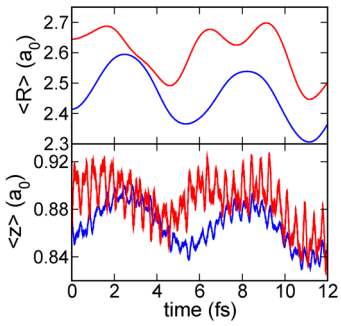

Figure 4. Same as Figure 3, but without laser pulse.

laser pulse is applied. The motion of the electronic wave packet is a superposition of (mostly) two oscillations: One rapid oscillation, due to the "sudden" displacement of the nuclei between propagations in imaginary time and real time, and a slower oscillation, which follows the nuclei almost adiabatically. If the EOM were linear, one could expect that the rapid oscillations would survive in Figure 3 to longer times. They are even faster than the electronic oscillations induced by the laser pulse, and should therefore not be affected by population transfer in lower lying levels. However, the expansion lengths used here still show a strong time-dependent state averaging[27] effect: The EOM change the orbitals in such a way that highly populated states are described more accurately, so that the population transfer during the first 4 fs leads to a decreasing amplitude on the highly excited states responsible for the quiver motion.

4. SUMMARY AND CONCLUSIONS

The simulations described in the previous section indicate that the influence of nuclear motion on the quantum dynamics of electrons is very small during the first 10 or so femtoseconds. This is especially so if the nuclei are initially in their ground state,

dx.doi.org/10.1021/jp304140r | J. Phys. Chem. A 2012, 116, 11107−11110

and need to acquire some momentum before they can lead to a dephasing of the electronic wave packet. Additionally, we find that the effect of nuclear motion is further suppressed if only a single SPF is used to represent the nuclear dof. This is equivalent to a mean field description, where the atoms cannot move in different ways on different potential energy surfaces. Accordingly, we found an almost 10-fold increase is the nuclear ampltitude when we increased the number of SPFs to two. This shows that higher expansion lengths would be required to obtain quantitative results, but unfortunately, the computational cost and a lack of numerical stability of our integrators prohibit simulations of that kind yet. Nevertheless, we believe that the results presented in the previous section give a good qualitative support for the fixed nuclei approximation for the time scales considered.

AUTHOR INFORMATION

Corresponding Author

*E-mail: mathias.nest@mytum.de.

Notes

The authors declare no competing financial interest.

ACKNOWLEDGMENTS

Financial support through the Deutsche Forschungsgemeinschaft through Grant Ne873/4-1 is gratefully acknowledged.

REFERENCES

(1) Tully, J. C.; Preston, R. K. Trajectory surface hopping approach to nonadiabatic molecular collisions: The reaction of H^+ with D_2. *J. Chem. Phys.* **1971**, *55*, 562−572.
(2) Tully, J. C. Molecular dynamics with electronic transitions. *J. Chem. Phys.* **1990**, *93*, 1061−1071.
(3) Drukker, K. Basics of surface hopping in mixed quantum/classical simulations. *J. Comput. Phys.* **1999**, *153*, 225−272.
(4) Deumens, E.; Diz, A.; Longo, R.; Öhrn, Y. Time-dependent theoretical treatments of the dynamics of electrons and nuclei in molecular systems. *Rev. Mod. Phys.* **1994**, *66*, 917−983.
(5) Broekhove, J.; Coutinho-Neto, M. D.; Deumens, E.; Öhrn, Y. Electron nuclear dynamics of LiH and HF in an intense laser field. *Phys. Rev. A* **1997**, *56*, 4996−5003.
(6) Deumens, E.; Öhrn, Y. Complete electron nuclear dynamics. *J. Phys. Chem. A* **2001**, *105*, 2660−2667.
(7) Killian, B. J.; Cabrera-Trujillo, R.; Deumens, E.; Öhrn, Y. Resonant charge transfer between H^+ and H from 1 to 5000 eV. *J. Phys. B* **2004**, *37*, 4733−4747.
(8) Cabrera-Troujillo, R.; Sabin, J. R.; Deumens, E.; Öhrn, Y. Cross sections for H^+ and H atoms colliding with Li in the low-keV-energy region. *Phys. Rev. A* **2008**, *78*, 012707.
(9) Seidner, L.; Stock, G.; Domcke, W. Nonperturbative approach to femtosecond spectroscopy: General theory and application to multidimensional nonadiabatic photoisomerization processes. *J. Chem. Phys.* **1995**, *103*, 3998−4011.
(10) Mahapatra, S.; Köppel, H.; Cederbaum, L. S. Reactive scattering dynamics on conically intersecting potential energy surfaces: The H + H_2 exchange reaction. *J. Phys. Chem. A* **2001**, *105*, 2321−2329.
(11) Klamroth, T.; Kröner, D.; Saalfrank, P. Laser-driven coupled electron−nuclear dynamics: Quantum mechanical simulation of molecular photodesorption from metal films. *Phys. Rev. B* **2005**, *72*, 205407.
(12) Rozgonyi, T.; Gonzalez, L. A two-dimensional wavepacket study of the nonadiabatic dynamics of CH_2BrCl. *J. Phys. Chem. A* **2008**, *112*, 5573−5581.
(13) Diestler, D. J.; Kenfack, A.; Manz, J.; Paulus, B. Coupled-channels quantum theory of electronic flux density in electronically adiabatic processes: Application to the hydrogen molecule ion. *J. Phys. Chem. A* **2012**, *116*, 2736−2742.
(14) Meyer, H.-D.; Manthe, U.; Cederbaum, L. S. The multi-configurational time-dependent Hartree approach. *Chem. Phys. Lett.* **1990**, *165*, 73−78.
(15) Beck, M. H.; Jäckle, A.; Worth, G. A.; Meyer, H.-D. The multi-configuration time-dependent Hartree method (MCTDH): A highly efficient algorithm for propagating wavepackets. *Phys. Rep.* **2000**, *324*, 1−105.
(16) Vendrell, O.; Gatti, F.; Meyer, H.-D. Full dimensional (15D) quantum-dynamical simulation of the protonated water dimer IV: Isotope effects in the infrared spectra of $D(D_2O)^{2+}$, $H(D_2O)^{2+}$, and $D(H_2O)^{2+}$ isotopologues. *J. Chem. Phys.* **2009**, *131*, 034308.
(17) Zanghellini, J.; Kitzler, M.; Fabian, C.; Brabec, T.; Scrinzi, A. An MCTDHF approach to multielectron dynamics in laser fields. *Laser Phys.* **2003**, *13*, 1064−1068.
(18) Kato, T.; Kono, H. Time-dependent multiconfiguration theory for electronic dynamics of molecules in an intense laser field. *Chem. Phys. Lett.* **2004**, *392*, 533−540.
(19) Nest, M.; Klamroth, T.; Saalfrank, P. The multi-configuration time-dependent Hartree−Fock method for quantum chemical calculations. *J. Chem. Phys.* **2005**, *122*, 124102.
(20) Remacle, F.; Nest, M.; Levine, R. D. Laser Steered Ultrafast Quantum Dynamics of Electrons in LiH. *Phys. Rev. Lett.* **2007**, *99*, 183902.
(21) Nest, M. The multi-configuration electron−nuclear dynamics method. *Chem. Phys. Lett.* **2009**, *472*, 171−174.
(22) Ulusoy, I. S.; Nest, M. The multi-configuration electron−nuclear dynamics method applied to LiH. *J. Chem. Phys.* **2012**, *136*, 054112.
(23) Haxton, D. J.; Lawler, K. V.; McCurdy, C. W. Multiconfiguration time-dependent Hartree−Fock treatment of electronic and nuclear dynamics in diatomic molecules. *Phys. Rev. A* **2011**, *83*, 063416.
(24) Szabo, A.; Ostlund, N.S. *Modern Quantum Chemistry*; Dover Publications: New York, 1989.
(25) Schmidt, M. W.; Baldridge, K. K.; Boatz, J. A.; Elbert, S. T.; Gordon, M. S.; Jensen, J. H.; Koseki, S.; Matsunaga, N.; Nguyen, K. A.; Su, S.; Windus, T. L.; Dupuis, M.; Montgomery, J. A. General atomic and molecular electronic structure system. *J. Comput. Chem.* **1993**, *14*, 1347−1363.
(26) Nest, M; Remacle, F.; Levine, R. D. Pump and probe ultrafast electron dynamics in LiH: A computational study. *New J. Phys.* **2008**, *10*, 025019.
(27) Padmanaban, R.; Nest, M. Origin of electronic structure and time-dependent state averaging in the multi-configuration time-dependent Hartree−Fock approach to electron dynamics. *Chem. Phys. Lett.* **2008**, *463*, 263−266.